Mater. Res. Soc. Symp. Proc. Vol. 1165 © 2009 Materials Research Society 1165-M04-01

The influence of the composition ratio on CZTS-based thin film solar cells

Hironori Katagiri, Kazuo Jimbo, Masami Tahara, Hideaki Araki and Koichiro Oishi
Nagaoka National College of Technology, 888 Nishikatakai, Nagaoka, Niigata 940-8532, Japan

ABSTRACT

Cu_2ZnSnS_4 (CZTS) thin films were fabricated by using three RF co-sputtering continued with sulfurization method. The new type of thin film solar cells using CZTS as an absorber consists of buffer-layer and window-layer on CZTS films that were fabricated on a Mo-coated soda-lime glass (SLG) substrate. It was confirmed that CZTS solar cells with high conversion efficiency existed in a relatively narrow composition region. In this paper, the fabrication method of CZTS-based thin film solar cells in our laboratory was stated briefly and the influence of the composition ratio on the photovoltaic properties were presented. Furthermore, the properties of a genuine non-toxic solar cell using a Cd-free buffer-layer were introduced.

INTRODUCTION

The low cost, environmental harmless Cu_2ZnSnS_4 (CZTS)-based thin film solar cells are fabricated by using abundant materials. The CZTS film possesses promising characteristic optical properties; band-gap energy of about 1.5 eV and large absorption coefficient in the order of 10^4 cm^{-1}. All constituents of this CZTS film, which are abundant in the crust of the earth, are non-toxic. Therefore, if we can use CZTS film practically as the absorber of solar cells, we will be free from both of the resource saving problem and the environmental pollution. K. Ito and we have reported the fabrication and the characterization of CZTS thin film solar cells [1-7]. In our laboratory, CZTS absorber layers were prepared by three RF sources co-sputtering technique followed by annealing in sulfurized atmosphere. The highest conversion efficiency of over 6.7 % was achieved by this method [6].

In our previous work, it was pointed out that those samples of Cu-poor and Zn-rich composition were preferable to improve the conversion efficiency. In order to clarify the region of composition ratio to achieve the high conversion efficiency, we fabricated solar cells with CZTS absorber layers having the wide range of composition ratio (Cu/(Zn+Sn); 0.75-1.25, Zn/Sn; 0.80-1.35). And we made the efficiency map which is corresponding to the composition ratio. As a result, it was confirmed that the solar cells with high conversion efficiency existed in a relatively narrow region in the map even in the range of Cu-poor and Zn-rich composition.

In the last section of this paper, an investigation of ZnO buffer-layer prepared by an Atmospheric Chemical-Vapor Deposition (A-CVD) method was introduced.

EXPERIMENT

A co-sputtering apparatus ULVAC-CS200A with an annealing chamber was used to fabricate CZTS thin films. Films were grown on soda-lime glass (SLG) substrates or Mo-coated one. The targets used in this study were Cu, ZnS and Sn or SnS. Those purities were all 99.99% with the exception of SnS of 99.9%. The parameters of precursor fabrication were as follows; Ar

gas flow rate: 50 sccm, Ar gas pressure: 0.5 Pa, Substrate rotation: 20 rpm, Pre-sputter time: 3 minutes, no substrate-heating. The precursors with various compositions were prepared by controlling each RF power. Then CZTS thin films were made by the sulfurization of precursors in annealing chamber, which is full of N_2+H_2S. The annealing temperature is ramped up from room temperature with the rate of 5°C/min up to 580 ^oC and it is retained for three hours. Then it is ramped down with the same rate until 200 ^oC followed by natural cooling. The heterojunction in the final solar cell consists of buffer-layer and window-layer on CZTS films. The buffer-layer was nearly always prepared by usual Chemical Bath Deposition (CBD) method. CdI_2 and thiourea were used as the Cd-source and S-source of CBD solution, respectively. The solution for CBD was prepared by mixing 400 ml of 0.42 mol CH_4N_2S aqueous solution, 50 ml of 0.04 mol CdI_2 aqueous solution and 110 ml of 28 % ammonium hydroxide solution. The CBD was carried out by soaking the SLG/Mo/CZTS in the mixture for 20 min, which was heated by hot-water bath of 70 ^oC. Then it was dried at 200 ^oC. The thickness of the CdS buffer layer was about 70 nm. ZnO:Al_2O_3 (2wt%) was used as the target in the sputtering system. The chemical compositions of the films were evaluated using X-ray Fluorescence Analysis (XRF) and Inductively Coupled Plasma-Optical Emission Spectrometry (ICP-OES). The structural characterization of the films was studied using X-ray Diffraction (XRD) analysis. The optical properties were measured by a photospectrometer. We estimated the cell properties of the CZTS solar cells from the *J-V* characteristic measured using a solar simulator. Furthermore, in order to produce the genuine non-toxic solar cells, we tried to apply ZnO films prepared by A-CVD to the new type of the buffer layer.

RESULTS AND DISCUSSION

Influence of H_2S concentration in the sulfurization

CZTS films were fabricated varying the concentration of H_2S to optimize the sulfurization ambience. In order to examine the influence of the concentration of H_2S upon the optical properties, the spectra of transmittance and reflectance of the CZTS films were measured by photospectrometer. Figure 1 shows the absorption coefficient spectra of the CZTS films. The concentration of H_2S has been changed from 5% to 20% in this experiment. Those inserted values in this figure refer to the concentration of H_2S in the atmosphere at the process of sulfurization. For all the samples, we can see that the CZTS thin films have the steep natures in the graphs of $(\alpha h\nu)^2$ - $(h\nu)$. It is inferred that CZTS is one of the direct transition semiconductor. By extrapolating these plots, we estimated the optical band gap energy of CZTS films as 1.5 eV which is very close to the optimum value for an absorber. This optical band gap energy has never changed with varying the concentration of H_2S. Furthermore, all the samples in this experiment have large absorption coefficients in the order of 10^4 cm^{-1} near a fundamental absorption edge. These optical properties show that this CZTS film is very suitable for an absorber of thin film solar cells. However, it is shown that the photo-absorption coefficient became smaller in the vicinity of $h\nu$=1.6 eV on the higher energy side in the case of 5% of H_2S.

Figure 2 shows X-ray diffraction (XRD) patterns of the CZTS films fabricated on SLG with the H_2S concentration of 5% and 20%. We can see no remarkable difference between these patterns. The composition of these films was almost stoichiometric (Cu/(Zn+Sn): 0.998-1.01 and Zn/Sn: 1.01-1.04) measured by ICP-OES. We can see some peaks due to (101), (112), (004), (200), (204), (220), (116) and (312) planes of CZTS, which are characteristic of the tetragonal

kesterite. From the XRD patterns, it can be confirmed that CZTS films of near stoichiometric composition have not any secondary phases such as binary and ternary compound.

Table I shows the comparison of the photovoltaic properties of CZTS-based thin film solar cells that were fabricated by the same batch process with the different concentrations of H_2S. There are no remarkable differences in the cell properties. As the results mentioned above, we can confirmed that there are no significant changes in the properties of CZTS films with respect to the concentration of H_2S in this region. Hereafter the concentration of H_2S is fixed to 5% to decrease the damage to the apparatus.

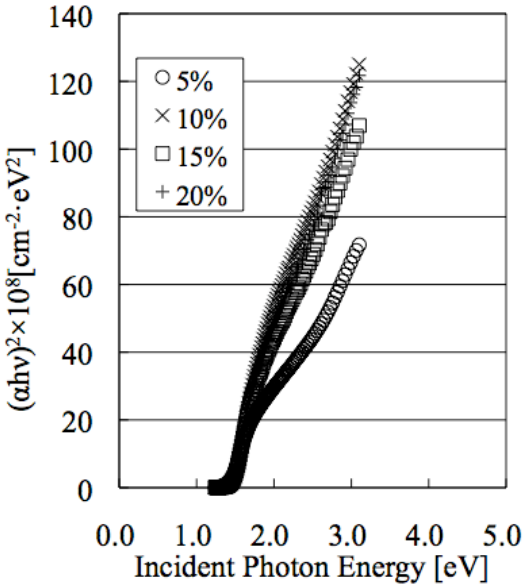

Figure 1. Comparison of the optical properties of CZTS films fabricated on SLG substrates using various concentrations of H_2S in the sulfurization process.

Table I. Comparison of the photovoltaic properties of CZTS-based thin film solar cells prepared by using different concentrations of H_2S in the sulfurization process.

Concentration of H_2S (%)	*Jsc* (mA/cm^2)	*Voc* (mV)	*FF*	Efficiency (%)
5.0	10.6	612	0.623	4.1
20	9.5	634	0.627	3.8

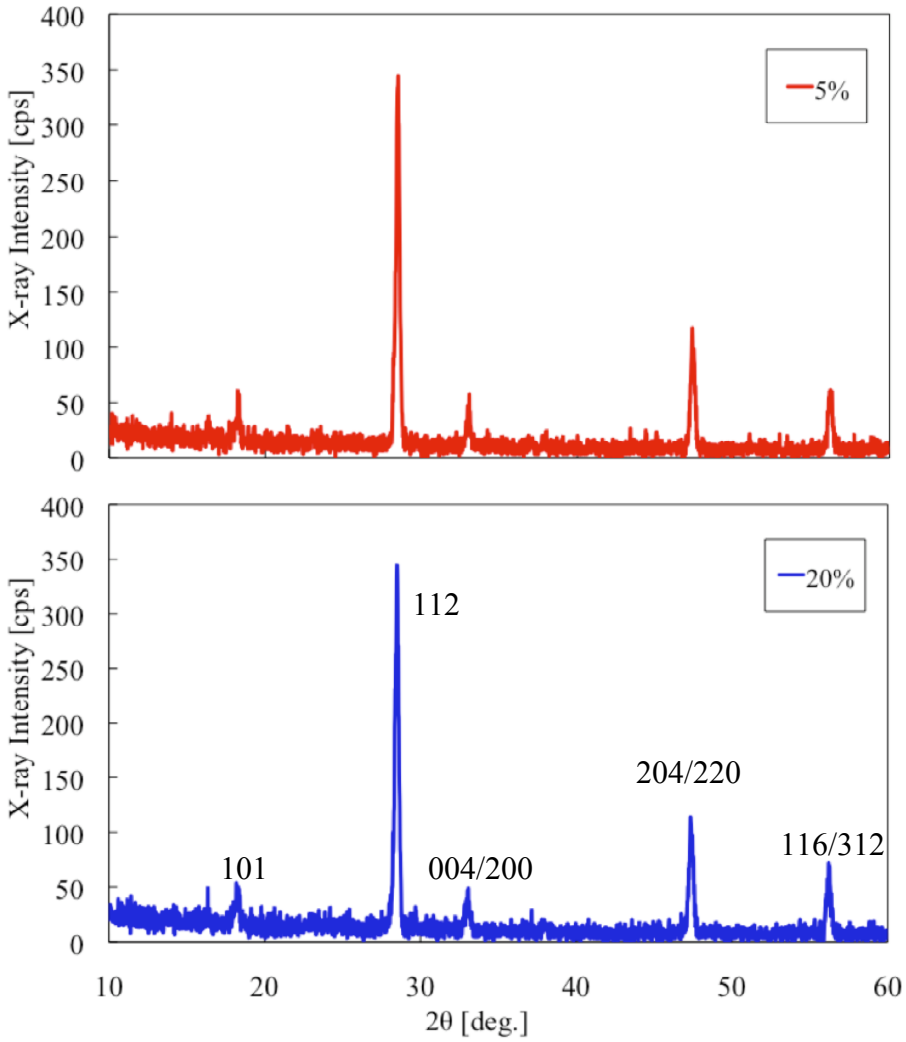

Figure 2. Comparison of XRD patterns of CZTS films prepared on SLG substrates by using different concentrations of H_2S in the sulfurization process.

Efficiency map on a pseudo-ternary phase diagram

In our previous works, the composition of the CZTS thin films exhibited high conversion efficiency showed Cu-poor and Zn-rich nature. In order to clarify the region of composition ratio to achieve the high conversion efficiency, we fabricated solar cells with CZTS absorber layers having the wide range of composition ratio (Cu/(Zn+Sn); 0.75-1.25, Zn/Sn; 0.80-1.35). Figure 3 shows the efficiency map corresponding to the composition ratio of Cu/(Zn+Sn) and Zn/Sn. In this map on the rectangular coordinates, the second quadrant refers to the area of Cu-poor and Zn-rich composition. It was confirmed that the solar cells with high conversion efficiency in this study existed in a relatively narrow region even in the area of Cu-poor and Zn-rich composition. The area looks like existing in a certain belt from the stoichiometry point toward the corner of the Cu-poor and Zn-rich composition in this figure.

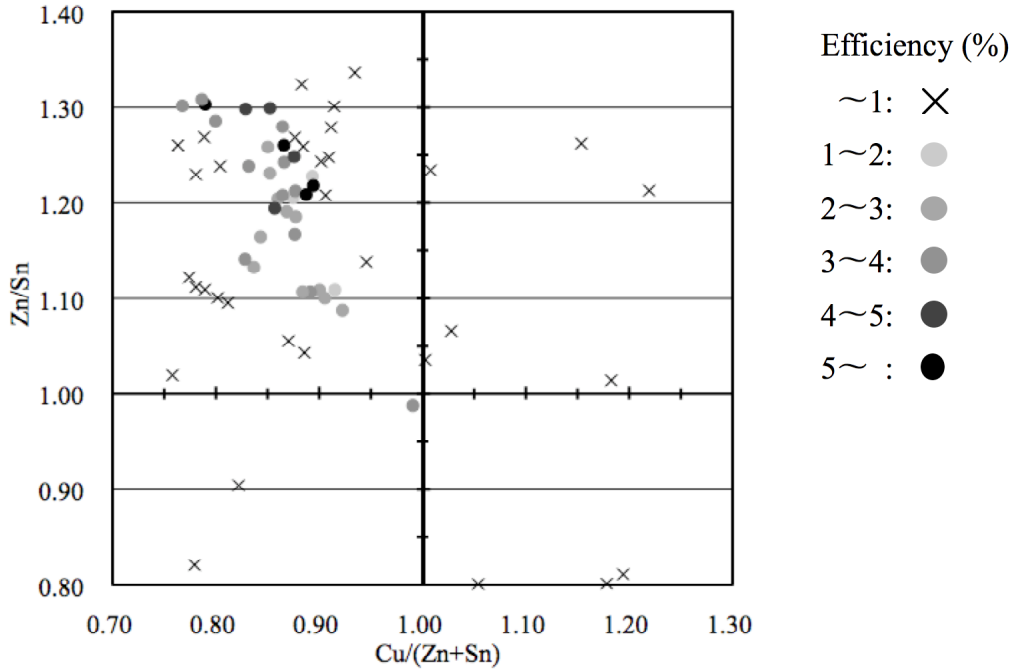

Figure 3. Conversion efficiency map of CZTS-based thin film solar cells on the rectangular coordinates of composition ratio of Cu/(Zn+Sn) and Zn/Sn. High conversion efficiency cells exist in a relatively narrow region in this figure.

Using the pseudo-ternary phase diagram of which CuS, ZnS and SnS are located at the corners of an equilateral triangle, we are able to remake the efficiency map. Th. M. Friedlmeier et. al. analyzed the structural properties of CZTS in detail with the similar pseudo-ternary ZnS-SnS_2-Cu_2S phase diagram [8]. Figure 4 shows the whole pseudo-ternary phase diagram that includes valuable information. The filled circle in the nearly middle of the map represents the pure CZTS, which consists of CuS of 50%, ZnS of 25% and SnS of 25%. On the green line between this filled circle and the corner of ZnS, the ratio of Cu/Sn is always stoichiometry of 2.0. If we assumed that all of the Cu and the Sn on this line are incorporated as CZTS, the excess Zn will be present as ZnS. Therefore, this green line represents a series of mixtures of x-CZTS and y-ZnS with an appropriate ratio. So the green line indicates the traces of (CZTS+ZnS). Similarly the opposite line of blue indicates the traces of (CZTS+Cu_2SnS_3). Two horizontal red lines show the traces of the samples of which the Cu/(Zn+Sn) ratio is 1.25 and 0.75, respectively. Similarly for the Zn/Sn ratio, two nearly vertical red lines from the corner of CuS represent the traces of 1.35 and 0.80, respectively. The region examined in this experiment was surrounded with these four red lines. Hereafter in order to clarify the influence of the composition ratio on photovoltaic properties in detail, we focused upon the inserted small orange triangle that includes the full area in this study.

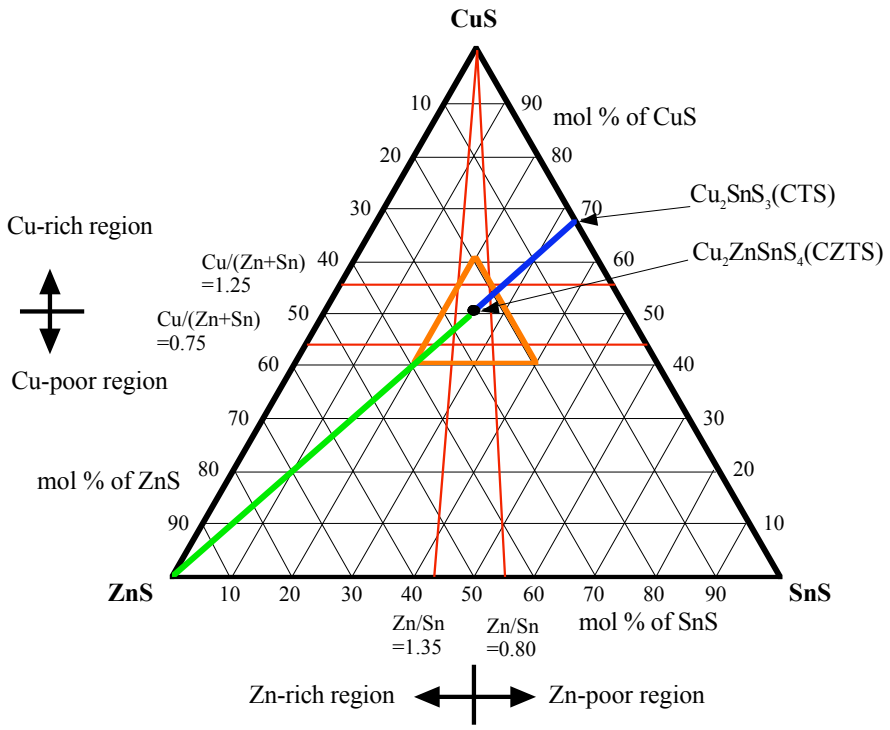

Figure 4. Pseudo-ternary phase diagram with CuS, ZnS and SnS. The filled circle in the nearly middle of the map represents CZTS, which consists of CuS of 50%, ZnS of 25% and SnS of 25%.

Figure 5 shows the efficiency map in the pseudo-ternary phase diagram using the data formerly indicated in figure 3. In this figure, the Cu-poor zone is under the bold horizontal line indicating the composition of CuS of 50%. Similarly, the Zn-rich films exist in a left half area separated by the bold vertical line. From this figure, we can see several important points. (1); there are no cells over 1% efficiency in the Cu-rich region. (2); even in the Cu-poor region, there are no effective cells in the area above the green (CZTS+ZnS) line. (3); even in the Cu-poor and Zn-rich region, there exists certain limit in the Sn concentration to keep the conversion efficiency high. In order to distinguish the reason to degrade the cell performance, an open-circuit voltage (*Voc*) and a short-circuit current density (*Jsc*) of each cell were shown in figure 6 and 7, respectively.

In figure 6, we can see that the green line indicates the compositional boundaries that separate the high-*Voc* cells from the others. There is no high-*Voc* cell in the upper side of the green line at all though we can see the dilution zone of various cells under the line. Since the ratio of Cu/Sn is larger than stoichiometry of 2.0, the excess Cu has to be present as CuS even though it is in the so-called Cu-poor region. In this upper side, there have to be CZTS, ZnS and excess CuS. CuS is well known as having semi-metallic nature. Therefore, the cells containing CuS have a tendency to degrade the *Voc* performance in this region. On the other hand, in figure 7, we can see that there are several cells with some *Jsc* above the green line. Because of the degraded *Voc* properties, we cannot achieve the high conversion efficiency in this region of which the excess CuS is present.

In figure 8, we can see what the externals of colloid formation on the CZTS surface after the CBD process looks like. The amount of the colloid increases with increasing the distance from the green line. In the left region separated by the vertical line drawn from the corner of CuS, the average composition in film is Zn-rich. But, in the region under the green line, there have to be CZTS, ZnS and excess SnS even though it is Zn-rich composition area. It is inferred that excess SnS enhanced the formation of colloidal CdS in CBD process and degraded the cell performance.

From the results mentioned above, in order to achieve the high conversion efficiency, we have to fabricate CZTS thin films in the narrow region alongside the green line. If the method for removing the semi-metallic CuS from the surface of CZTS films was accomplished, the window of production condition will be widened. Similarly, the optimization of the buffer-layer is quite important to prevent the degradation of *Voc*.

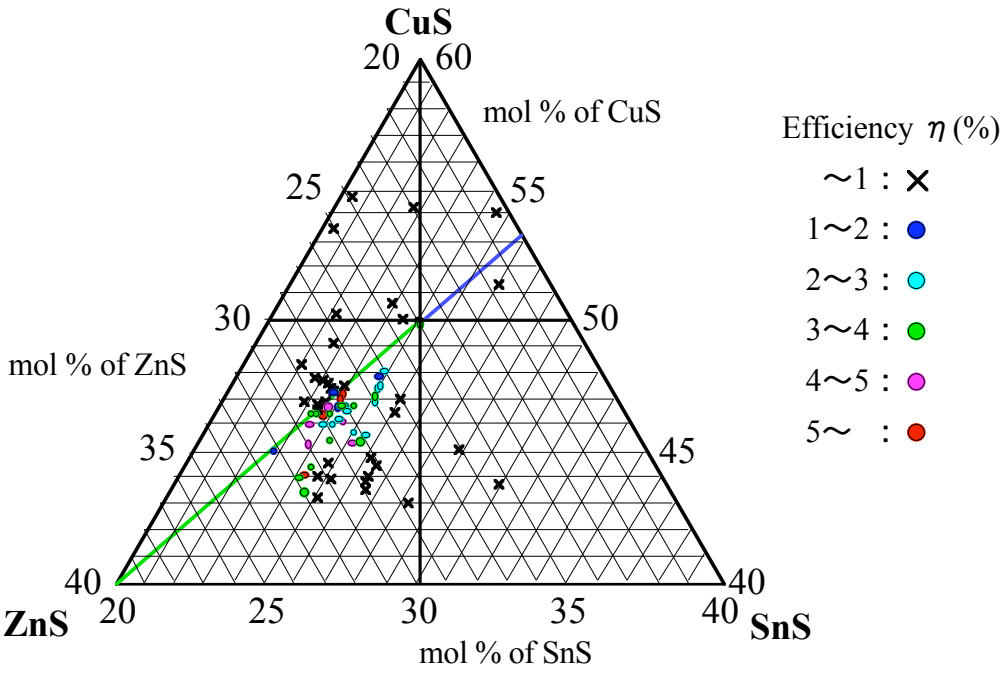

Figure 5. Efficiency map on the pseudo-ternary phase diagram. The green line looks like a boundary between the high conversion efficiency cells and the others.

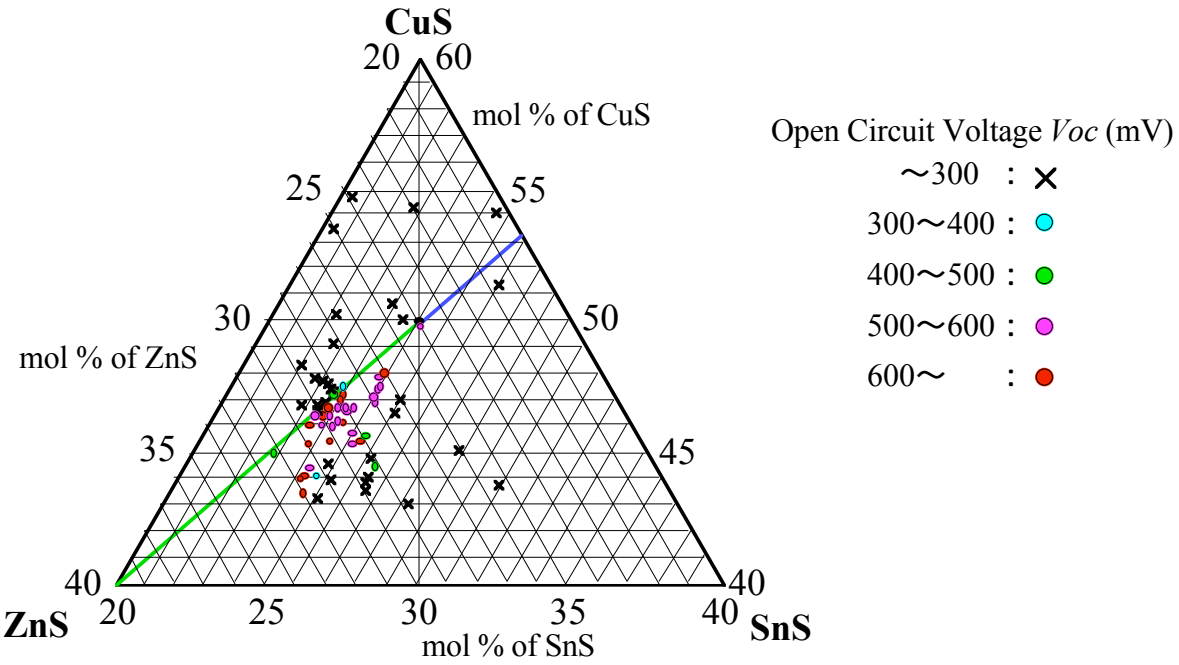

Figure 6. Open Circuit Voltage *Voc* map on the pseudo-ternary phase diagram. There are no high-*Voc* cells above the green line.

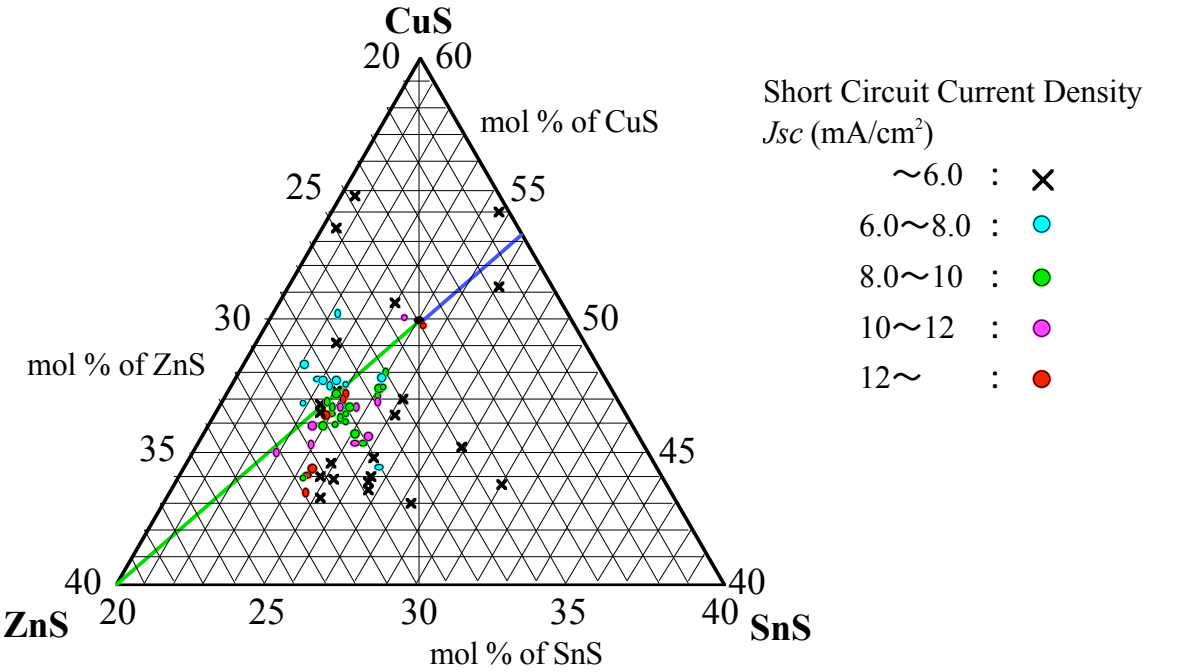

Figure 7. Short Circuit Current Density *Jsc* map on the pseudo-ternary phase diagram. We can see the cells above the green line exhibiting some *Jsc*.

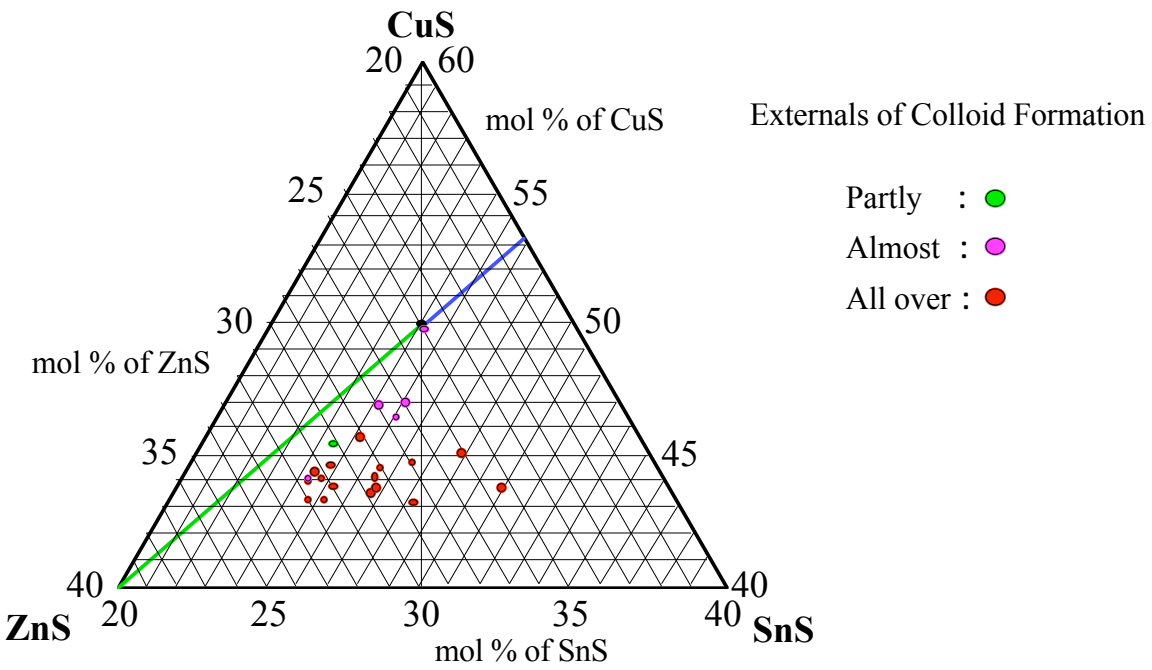

Figure 8. Externals of colloid formation on the CZTS surface after the CBD process. The amount of the colloid increases with increasing the distance from the green line.

Investigation of Cd-free buffer layer

In order to produce the genuine non-toxic solar cells, we tried to apply ZnO film to the buffer layer instead of CBD-CdS. ZnO films were prepared by an Atmospheric Chemical-Vapor Deposition (A-CVD) apparatus of which name is Type A314-03 provided TOKITA CVD Systems Co. Ltd. Figure 9 shows a schematic diagram of the A-CVD apparatus we used. The raw material used to prepare ZnO film was coordination compounds in this system. In this study, $Zn(C_5H_7O_2)_2$ (Soekawa Chemical, quoted purity of 99.9%) was used. This reactant was loaded into a vaporizer and vaporized at 125 ^oC. The reactant vapor was first carried by N_2 flowing at a rate of 3.0 liter/min and then sprayed from the metallic nozzle directly onto CZTS fabricated on Mo-coated SLG substrate. The substrate was heated up to 200-350 ^oC using the mounted electric heater. The reactant was immediately decomposed by the thermal energy from the substrate heater to form ZnO films. The distance between the nozzle and the substrate was fixed at 20 mm in this study. The substrate holder was reciprocated horizontally and passed 4 times under the nozzle at the velocity of 4.6 mm/sec. ZnO films with the thicknesses of about 60 nm were formed by this technique.

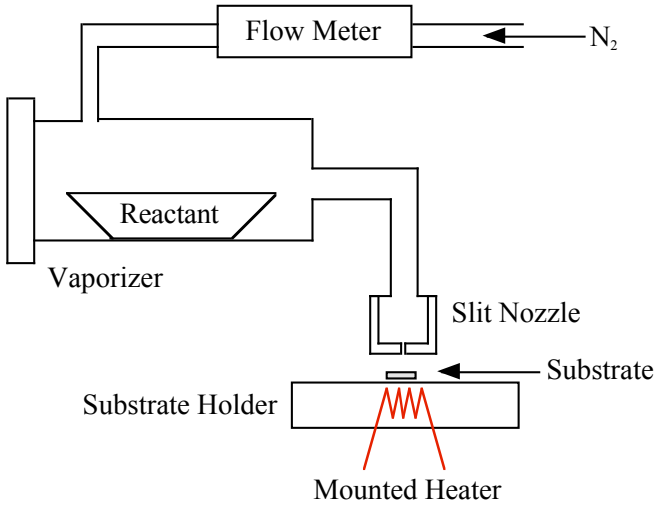

Figure 9. Schematic diagram of A-CVD apparatus used in this study.

Figure 10 and 11 show *J-V* characteristics and external quantum efficiency observed by the genuine rare metal-free and Cd-free thin film solar cells, respectively. In figure 10, the sample of which substrate temperature was 250 ^{o}C showed the open-circuit voltage of 623 mV, the short-circuit current density of 13.9 mA/cm^2, the fill factor of 0.6 and the highest conversion efficiency of 5.19% in this study. With increasing the substrate temperature, the short-circuit current density increased without the case of 350 ^{o}C while the open-circuit voltage decreased. In figure 11, the shape of each spectral response was similar with the exception of the one of 350 ^{o}C. This change was mainly caused by Zn diffusion into CZTS film under the condition of high substrate temperature of 350 ^{o}C. For the cells prepared beneath 300 ^{o}C, we can't see the decrease of response around 500 nm. This is the clear evidence that these cells were fabricated without CdS buffer layer. In order to increase the conversion efficiency, several investigations are in progress.

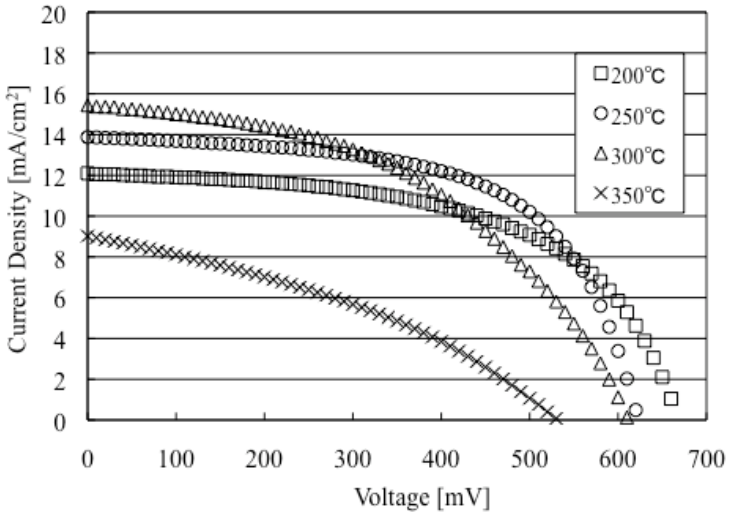

Figure 10. Comparison of *J-V* characteristics with various temperatures. The inset refers to the substrate temperature during deposition period of ZnO buffer layer.

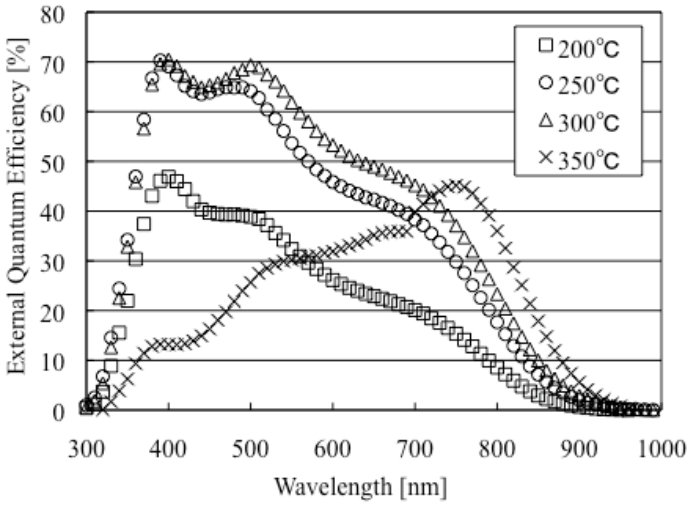

Figure 11. Comparison of external quantum efficiency with various temperatures. The inset refers to the substrate temperature during deposition period of ZnO buffer layer.

CONCLUSIONS

We first report the conversion efficiency map of CZTS-based thin film solar cells using the pseudo-ternary CuS-ZnS-SnS phase diagram. It is confirmed that the excess CuS degrade the *Voc* properties and the excess SnS results in the formation of the colloidal CdS in the CBD process. In order to achieve the high conversion efficiency, we have to fabricate CZTS thin films in the narrow region even though in the area of Cu-poor and Zn-rich composition.

Furthermore, the new type of buffer layer prepared by the A-CVD method, instead of CBD-CdS, is introduced to produce the genuine rare-metal free and non-toxic thin film solar cells. Because of this dry-process, we will be free from the disposal problem of chemical solutions.

REFERENCES

1. K. Ito, T. Nakazawa, Jpn. J. Appl. Phys. **27**, 2094 (1988).
2. H. Katagiri, K. Saitoh, T. Washio, H. Shinohara, T. Kurumadani, S. Miyajima, Sol. Energy Mater. Sol. Cells **65**, 141 (2001).
3. H. Katagiri, N. Ishigaki, T. Ishida, K. Saitoh, Jpn. J. Appl. Phys. **40**, 500 (2001).
4. H. Katagiri, Thin Solid Films **480-481**, 426 (2005).
5. K. Jimbo, R. Kimura, T. Kamimura, S. Yamada, W. S. Maw, H. Araki, K. Oishi, H. Katagiri, Thin Solid Films **515**, 5997 (2007).
6. H. Katagiri, K. Jimbo, S. Yamada, T. Kamimura, W. S. Maw, T. Fukano, T. Ito, T. Motohiro, Appl. Phys. Express **1**, 041201 (2008).
7. H. Katagiri, K. Jimbo, W. S. Maw, K. Oishi, M. Ymazaki, H. Araki, A. Takeuchi, Thin Solid Films **517**, 2455 (2009).
8. Th. M. Friedlmeier, PhD Thesis, University of Stuttgart (2001), p.39-43.